Alternative drug-response metric based on cellular response phenotypes

Sanghyun Kim[1*] and Sohyun Hwang[1,2*]

[1] Department of Biomedical Science, College of Life Science, CHA University, 335 Pangyo-ro, Sungnam 13488, South Korea

2 Department of Pathology, CHA Bundang Medical Center, 65-11 Yatap-ro, Seongnam 13496, South Korea

* Correspondence: Kim mudol@chauniv.ac.kr, Hwang blissfulwin@cha.ac.kr

ABSTRACT

Current drug-response metrics based on viability or apparent growth rates are limited by their dependency on the assay duration and lack of reflections regarding actual cellular drug-response phenotypes. To resolve these limitations, we evaluated the contribution of each cellular response phenotype to a drug on the overall growth behavior. This provides a time-independent phenotype metric which can reveal the mechanisms underlying growth inhibition of specific cells by a given drug.

MAIN TEXT

Drug responses in cultured cell lines are essential for identifying molecular variants associated with the therapeutic effectiveness of the drug, mostly through integration with large genomic data[1–6]. For better pharmacogenomic analyses, two limitations need to be addressed adequately: the issue of irreproducibility in drug-response studies, and the existing discordance between actual cellular response phenotypes and conventional drug-response metrics. Concerns regarding reproducibility in drug-response studies are widespread and have been raised repeatedly in preclinical studies[7–9]. In contrast, the second limitation is a more general issue; while actual response phenotypes during drug treatment are diverse—including

senescence and various forms of programmed cell death—conventional metrics such as IC_{50} (half maximal inhibitory concentration) do not reflect such responses. Instead, these metrics are simply *de facto* standards for crudely categorizing cell lines as either sensitive or resistant without an underlying theoretical basis.

A recent multi-center study of the NIH Library of Network-Based Cellular Signatures Program (LINCS) on drug-response assays[10] well evaluated the irreproducibility issue. A notable point of this study was that the cell growth rate[11,12]—instead of viability—was used as a metric for characterizing drug responses. In general, normal cell growth is an exponential function of time; however, cell growth is inhibited by drugs. The difference in cell viability between drug-treated and -untreated conditions increases with time; that is, a longer treatment duration results in lower cell viability. This tendency becomes more prominent with an increase in dosage; hence, the longer the assay duration, the lower the IC_{50}. Along with this inconsistency based on the assay duration, a viability-based metric has an additional limitation with respect to comparing the drug responses of various cell lines, because each cell line—with its own doubling time—is differently influenced by the same treatment duration. Thus, a viability-based metric cannot provide consistent criteria regarding which cells are sensitive or resistant to treatment with a certain drug. To correct for these confounders, alternative metrics based on the growth rate, such as drug-induced-proliferation rate[11] or growth rate (GR)[12], have been suggested. Indeed, the GR metric reportedly improved the reproducibility and performance of pharmacogenomic association studies[13].

However, such growth-rate-based metrics have also been shown to be time-dependent in numerous cases, as observed in the MCF10A cell line treated with neratinib in the LINCS study[10]. This implies that cellular growth behavior is not a simple exponential function such as $N(t) = N_0 e^{kt}$. The common assumption regarding cell growth as a simple exponential function results from the premise that the rate of changes in cell number is proportional to the present number of cells. The proportional factor is a growth rate, k. However, if some of the viable cells are undergoing cell cycle arrest—which does not contribute to changes in the cell count—viable cells do not follow simple exponential growth. The number of proliferating cells itself might be an exponential function; however, the total number of viable cells (including both proliferating cells and cell cycle-arrested cells) is not. This finding indicates the need for considering the actual cellular response phenotypes when evaluating drug responses.

Therefore, we investigated how each cellular drug-response phenotype contributes to the overall growth behavior. Phenotypes can be simply divided into three groups based on cell division and viability;

proliferation, death, and cell cycle arrest (i.e., senescence). Senescence has never emerged in previous metrics of the drug response, but is a widely reported phenomenon known as therapy-induced senescence[14–16]. Population dynamics can be easily determined; the number of cells with each phenotype (N_p proliferating cells, N_s senescent cells, and N_d dead cells) changes only by cell division (with rate of change, k_p) or cell death (k_d), or due to cell cycle arrest (s) among proliferating cells (Fig. 1a). Accordingly, the complete differential equations are given as shown in Fig. 1c, and their solutions can be obtained analytically. The death of senescent cells has been disregarded herein ($s_d \sim 0$), the exception being the coexistence of senolytic drugs or immune cells.

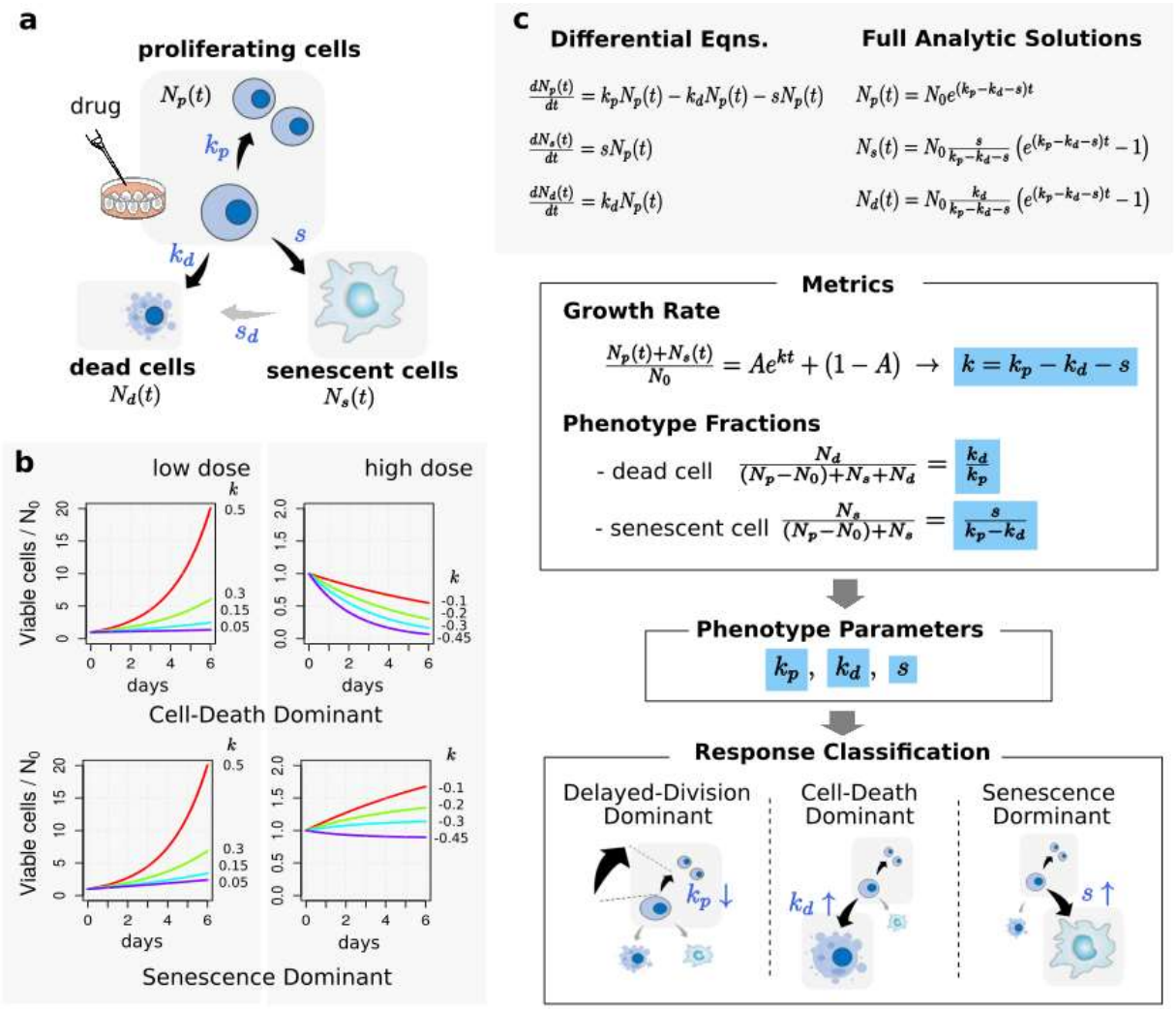

Figure 1 Cellular drug-response phenotype-metrics. (a) Schematic illustration of the cellular response phenotype during drug treatment. Proliferating cells can continue dividing, can enter a state of permanent cell cycle arrest, or can undergo cell death. (b) Typical growth curves representing viability as a function of time in either cell death-dominant or senescence-dominant conditions. Two drug concentration ranges are considered because of the large difference in the scale of the y-axis displaying the number of viable cells; the low dose corresponds to a point where the proliferating growth rate is positive, and the high dose corresponds to the point where the rate is negative. Detailed values of these parameters are provided in Supplementary Table 1. (c) The evaluation steps of phenotype metrics for drug responses. The different drug-response metrics are compared in Supplementary Table 2.

The explicit functional form of the solution reveals several interesting points. First, the system contains only one characteristic exponent: the growth rate of the proliferating cells ($k = k_p - k_d - s$). Recent advancements in time-lapse imaging in live cell microscopy[17] potentially provide a useful platform for measuring the cellular kinetics to determine the growth rate. However, unless specifically enumerating the proliferating cells, a proper fitting function should be applied to the number of viable cells ($\frac{N_p+N_s}{N_0} = Ae^{kt} + 1 - A$) or dead cells ($\frac{N_d}{N_0} = B(e^{kt} - 1)$) to determine the proliferating -growth-rate. A simple exponential fitting ($N(t) = N_0 e^{k't}$) for the viable cell count—which is considered for the growth-rate-based metric—would yield an apparent growth rate varying on the basis of the assay duration. Herein, time dependency of the apparent growth rate would be intrinsic because of the senescent cell subpopulations rather than because of other confounders. Indeed, significant induction of senescence[16,18] has been observed in cases displaying time-dependent GRs [10–12], such as following the treatment of MCF10A cells with neratinib.

Second, the proliferating-growth-rate alone cannot indicate whether growth inhibition results from the delay in cell division (k_p reduction), promotion of cell death (k_d increase), or cell cycle arrest (s increase). At high doses, the typical growth curves of viable cells (Fig. 1b) displayed minor differences between the cell death-dominant and senescence-dominant conditions; a small increase in a saturated manner for the senescence-dominant condition and an exponential reduction in the cell death-dominant condition. However, such differences are too small relative to the scale of changes displayed in low-dose curves to determine which inhibition mechanism is dominant for a certain drug–cell line pair from the overall growth behavior. In fact, we need to know the value of each parameter (k_p, k_d, and s)—not only the overall growth rate—to determine the mechanism underlying growth inhibition. Fortunately, the phenotype fractions of senescence and cell death are given as simple parameter ratios; accordingly, measurement of the phenotype fractions along with the proliferating-growth-rate would enable the determination of the parameters, and therefore the underlying mechanism (Fig. 1c).

These findings were confirmed during actual data evaluation. We used a publicly available dataset including both time-lapse enumerations of viable cells and end-point measurements of the phenotype fractions. The ovarian cancer cell lines OV1369(R2) and OV1946 were treated with the PARP inhibitor olaparib[19]. The viability and GR metrics displayed significant differences between 3-d and 6-d assays, indicating their time-dependency (Fig. S1 and Supplementary Table 3a, b). IC_{50} and GR_{50} values of 6-d assays were much lower than those of 3-d assays (1.5–3 times for OV1369(R2) and ~10 times for OV1946);

thus, these metrics cannot serve as a consistent criterion for drug potency. However, the phenotype metric provides the actual proliferating-growth rate, not an apparent time-dependent growth-rate, along with the actual value for each parameter. The proliferating-growth rate was lower than half of the normal growth rate even upon treatment of olaparib with 2.5 μM for OV1369(R2) cells and 0.01 μM for OV1946 cells (Fig. 2a). These concentrations were markedly lower than the reported IC_{50} (10 μM for OV1369(R2) cells and 0.1 μM for OV1946 cells)[19]. At this concentration, OV1396(R2) cells displayed a marked reduction in k_p (-47%), negligible alteration in k_d (0%), and a slight increase in s (10%), implying that senescence is dominant upon olaparib treatment in addition to delayed cell division. However, OV1946 cells displayed a slight reduction in k_p (-28%) and an increase in k_d (26%), but only showed a slight increase in s (4%) (Fig. 2b). These findings indicate that for OV1946 cells, not only is growth significantly inhibited even at a low dose of olaparib, but that this effect results from cell death rather than senescence. Another advantage of this phenotype metric is that a single-concentration assay at clinically relevant levels can adequately determine the drug potency and the dominant mechanism underlying growth inhibition. In general, conventional metrics require a full-concentration-range assay to determine the IC_{50}.

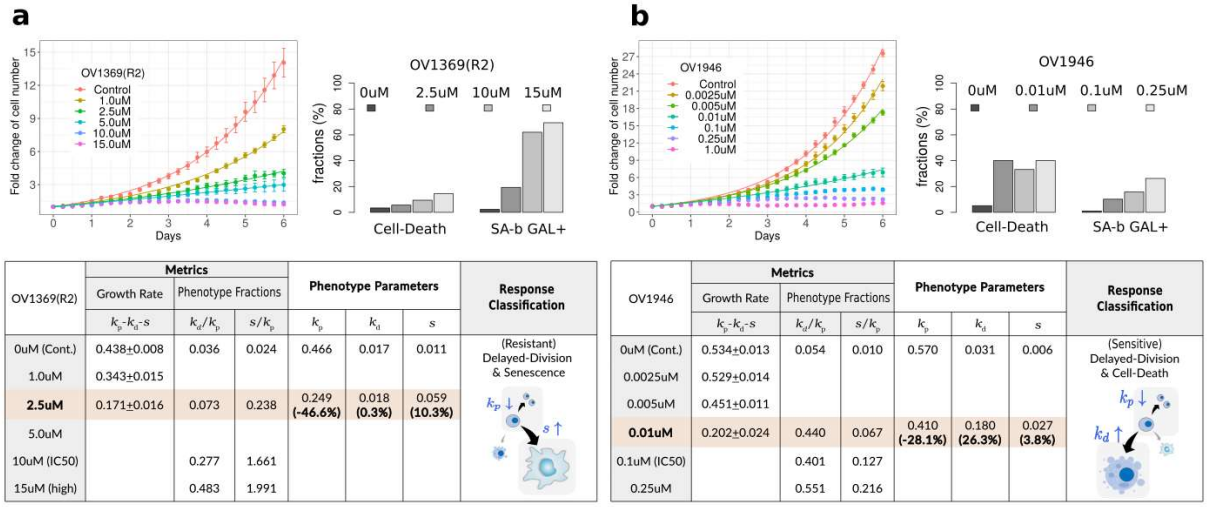

OV1369(R2)	Metrics: Growth Rate	Metrics: Phenotype Fractions		Phenotype Parameters			Response Classification
	k_p-k_d-s	k_d/k_p	s/k_p	k_p	k_d	s	
0uM (Cont.)	0.438±0.008	0.036	0.024	0.466	0.017	0.011	(Resistant) Delayed-Division & Senescence
1.0uM	0.343±0.015						
2.5uM	0.171±0.016	0.073	0.238	0.249 **(-46.6%)**	0.018 **(0.3%)**	0.059 **(10.3%)**	
5.0uM							
10uM (IC50)		0.277	1.661				
15uM (high)		0.483	1.991				

OV1946	Metrics: Growth Rate	Metrics: Phenotype Fractions		Phenotype Parameters			Response Classification
	k_p-k_d-s	k_d/k_p	s/k_p	k_p	k_d	s	
0uM (Cont.)	0.534±0.013	0.054	0.010	0.570	0.031	0.006	(Sensitive) Delayed-Division & Cell-Death
0.0025uM	0.529±0.014						
0.005uM	0.451±0.011						
0.01uM	0.202±0.024	0.440	0.067	0.410 **(-28.1%)**	0.180 **(26.3%)**	0.027 **(3.8%)**	
0.1uM (IC50)		0.401	0.127				
0.25uM		0.551	0.216				

Figure 2 | Phenotype metric-based evaluation of ovarian cancer cell lines (a) OV1369(R2) and (b) OV1946 treated with olaparib. Fold change values of viable cells and the fraction of dead and senescent cells are re-plotted using publicly available raw data (upper), and phenotype metrics were evaluated as indicated in Fig. 1c (lower table).

Reliable drug-response data are critical in preclinical pharmacology. The recent growth-rate-based metrics facilitated better evaluation of drug responses than previously used viability-based metrics. However, these metrics are based on the assumption that overall growth is a simple exponential function, which is not always true. Potential confounders can still not be avoided when assessing the resulting apparent growth

rate. This can be resolved through the time-lapse enumeration of only proliferating cells among the total viable cells or by appropriately fitting the model to total viable cells, as proposed herein. Moreover, the rate of changes for proliferating cells to each phenotype can be determined by measuring the phenotype fractions along with the proliferating-growth-rate. Such considerations of response phenotypes make a drug-response metric intuitive and biologically interpretable, and the ability to determine the mechanism underlying growth inhibition would be markedly improved upon pharmacogenomic analysis.

ACKNOWLEDGMENTS

This research was supported by Basic Science Research Program through the National Research Foundation of Korea (NRF) funded by the Ministry of Education (No. NRF-2019R1A6A1A03032888) and by a grant (HI16C1559) from the Korea Health Technology R&D Project through the Korea Health Industry Development Institute (KHIDI), funded by the Ministry of Health & Welfare, Republic of Korea.

AUTHOR CONTRIBUTIONS

S. K. and S. H. conceived the idea and wrote the manuscript. S. K. built and evaluated the mathematical models and analyzed the public data. S. H. supervised the study.

COMPETING FINANCIAL INTERESTS

The authors declare no competing financial interests.

REFERENCES

1. Barretina, J. *et al.* The Cancer Cell Line Encyclopedia enables predictive modelling of anticancer drug sensitivity. *Nature* **483**, 603–607 (2012).
2. Wang, L., McLeod, H. L. & Weinshilboum, R. M. Genomics and Drug Response. *N. Engl. J. Med.* **364**, 1144–1153 (2011).
3. Garnett, M. J. *et al.* Systematic identification of genomic markers of drug sensitivity in cancer cells. *Nature* **483**, 570–575 (2012).
4. Costello, J. C. *et al.* A community effort to assess and improve drug sensitivity prediction algorithms. *Nat.*

Biotechnol. **32**, 1202–1212 (2014).

5. Rees, M. G. *et al.* Correlating chemical sensitivity and basal gene expression reveals mechanism of action. *Nat. Chem. Biol.* **12**, 109–116 (2016).
6. Iorio, F. *et al.* A Landscape of Pharmacogenomic Interactions in Cancer. *Cell* **166**, 740–754 (2016).
7. Collins, F. S. & Tabak, L. A. Policy: NIH plans to enhance reproducibility. *Nat. News* **505**, 612 (2014).
8. Freedman, L. P., Cockburn, I. M. & Simcoe, T. S. The Economics of Reproducibility in Preclinical Research. *PLOS Biol.* **13**, e1002165 (2015).
9. Haibe-Kains, B. *et al.* Inconsistency in large pharmacogenomic studies. *Nature* **504**, 389–393 (2013).
10. Niepel, M. *et al.* A Multi-center Study on the Reproducibility of Drug-Response Assays in Mammalian Cell Lines. *Cell Syst.* **9**, 35-48.e5 (2019).
11. Harris, L. A. *et al.* An unbiased metric of antiproliferative drug effect in vitro. *Nat. Methods* **13**, 497–500 (2016).
12. Hafner, M., Niepel, M., Chung, M. & Sorger, P. K. Growth rate inhibition metrics correct for confounders in measuring sensitivity to cancer drugs. *Nat. Methods* **13**, 521–527 (2016).
13. Hafner, M., Niepel, M. & Sorger, P. K. Alternative drug sensitivity metrics improve preclinical cancer pharmacogenomics. *Nat. Biotechnol.* **35**, 500–502 (2017).
14. Ewald, J. A., Desotelle, J. A., Wilding, G. & Jarrard, D. F. Therapy-Induced Senescence in Cancer. *JNCI J. Natl. Cancer Inst.* **102**, 1536–1546 (2010).
15. Mikuła-Pietrasik, J., Niklas, A., Uruski, P., Tykarski, A. & Książek, K. Mechanisms and significance of therapy-induced and spontaneous senescence of cancer cells. *Cell. Mol. Life Sci.* **77**, 213–229 (2020).
16. Wang, B., Kohli, J. & Demaria, M. Senescent Cells in Cancer Therapy: Friends or Foes? *Trends Cancer* **6**, 838-857 (2020).
17. Gelles, J. D. *et al.* Single-Cell and Population-Level Analyses Using Real-Time Kinetic Labeling Couples Proliferation and Cell Death Mechanisms. *Dev. Cell* **51**, 277-291.e4 (2019).
18. McDermott, M. S. J. *et al.* HER2-Targeted Tyrosine Kinase Inhibitors Cause Therapy-Induced-Senescence in Breast Cancer Cells. *Cancers* **11**, 197 (2019).
19. Fleury, H. *et al.* Exploiting interconnected synthetic lethal interactions between PARP inhibition and cancer cell reversible senescence. *Nat. Commun.* **10**, 2556 (2019).

ONLINE METHODS

Public Data Drug-response data were obtained from the source data file of Fleury[19] (https://www.nature.com/articles/s41467-019-10460-1#Sec32). This was the only publicly available dataset to date that included both time-lapse enumerations of viable cells and the end-point measurements of the phenotype fractions. The phenotype metric was evaluated for the data of OV1369(R2) and OV1946 cells treated with olaparib. All data analyses and plots of the typical growth curve were performed in R (version 3.6.1).

Typical Growth Curve Based on the Phenotype Model of Drug Response. The viable cell number as a function of time was plotted for different parameter values (k_p, k_d, s) in the case of either cell death-dominant or senescence-dominant conditions (Fig. 1c). It was assumed that k_d (for the cell death-dominant condition) or s (for the senescence-dominant condition) increases gradually with an increase in the drug concentration, but with a similar reduction in k_p. Because the fold change in the viable cell number varies largely depending on the proliferating-growth- rate $(k = k_p - k_d - s)$, we divided the dose range into two, in which the proliferating-growth-rate is positive with a low dose and is negative with a high dose. The intrinsic doubling time of the cells (i.e., no drug treatment) was assumed to be ~1.4 d, corresponding to k_p = 0.5. Detailed values of the parameters for the plot in Fig. 1c are provided in Supplementary Table S1.

Phenotype Metric 1: Proliferating Growth Rate by Fitting Kinetic Measurements. The viable cell counts, divided by the initial number N_0, were fit with a 2-parameter exponential function, $Ae^{kt} + (1 - A)$, using nonlinear least-squares regression. Fitting was performed using the "nls" function within the R statistical programming environment, and the proliferating-growth-rate, k, is presented as one of the fitting parameters (Fig. 2). For comparison, the apparent growth rate was determined through the simple exponential function e^{Bt}, using either a 3-d or 6-d fitting range (a schematic representation of the evaluation and the results of the drug-response metrics are provided in Supplementary Table 2 and Supplementary Table S3, respectively).

Phenotype Metric 2: Phenotype Fraction. Phenotype fractions are calculated as $\frac{N_s}{N_p - N_0 + N_s} = \frac{s}{k_p - k_d}$ for senescent cells and as $\frac{N_d}{N_d - N_0 + N_s + N_d} = \frac{k_d}{k_p}$ for dead cells according to the explicit functional form of each phenotypic growth. Note that $N_p - N_0$, instead of N_p, makes the fractions a simple ratio of the parameters.

However, the phenotype fractions in the used public data were obtained in the conventional forms through either the SA beta-galactosidase assay ($\frac{N_s}{N_p+N_s}$) or flow cytometry ($\frac{N_d}{N_p+N_s+N_d}$). To convert the conventional form to the form of a simple ratio, $\mathrm{FC} = \frac{N_p+N_a}{N_0}$ was obtained from the kinetic measurements and used as $\frac{N_s}{N_p-N_0+N_s} = \frac{N_s}{N_p+N_s}\frac{\mathrm{FC}}{\mathrm{FC}-1}$ and $\frac{N_d}{N_p-N_0+N_s+N_d} = \frac{\frac{N_d}{N_p+N_s+N_d}\mathrm{FC}}{\mathrm{FC}-1+\frac{N_d}{N_p+N_s+N_d}}$.

Phenotype Parameter and Response Classification The actual values of k_p, k_d, and s were determined from $k_p - k_d - s$, $\frac{N_d}{N_{d-}N_0+N_s+N_d} = \frac{k_d}{k_p}$, and $\frac{N_s}{N_p-N_0+N_s} = \frac{s}{k_p-k_d}$. Thereafter, at a certain drug concentration, each parameter value can be represented by the extent of its variation relative to $k_p(0)$, the proliferating-growth rate upon no drug treatment, such as by the percent change of $k_d = \frac{k_d(C)-k_d(0)}{k_p(0)}$. By comparing the percent change of each parameter, a dominant mechanism underlying growth inhibition could be determined.

SUPPLEMENTARY FIGURE AND TABLES

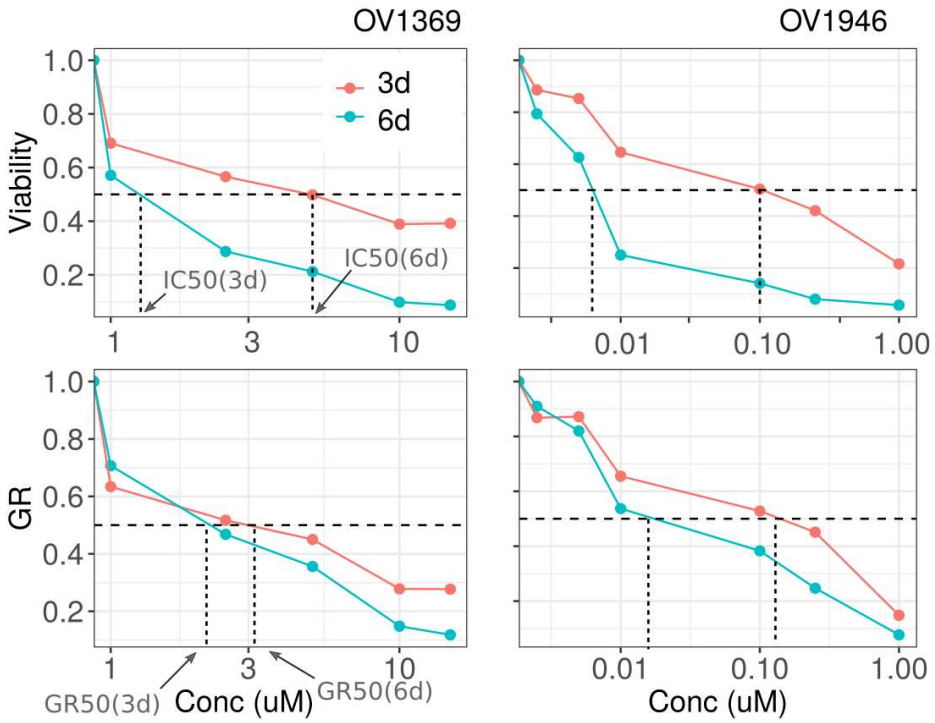

Supplementary Figure 1. Time dependence of the conventional metrics.

Viability and GR for different assay durations (3-d and 6-d) were compared for OV1369(R2) and OV1946 cells respectively. Detailed values of each metric evaluation are in Supplementary Table 3. Clearly 6-d assay displayed a lower viability in the full concentration range. For GR metric, there was a crossover between two assays in a certain point in a low concentration range. Lower apparent growth rates for 6-d assays than 3-d assays became clear above the crossover point, and that would be because a population of senescent cells became a significant portion with time above a certain concentration.

	Cell-death Dominant								Senescence Dominant							
k_p	0.5	0.4	0.3	0.25	0.2	0.15	0.1	0	0.5	0.4	0.3	0.25	0.2	0.15	0.1	0
k_d	0	**0.1**	**0.15**	**0.2**	**0.3**	**0.35**	**0.4**	**0.45**	0	0.05	0.05	0.05	0.05	0.05	0.05	0.05
s	0	0	0	0	0	0	0	0	0	**0.05**	**0.1**	**0.15**	**0.25**	**0.3**	**0.35**	**0.4**
Proliferating -growth-rate $k_p - k_d - s$	0.5	0.3	0.15	0.05	-0.1	-0.2	-0.3	-0.45	0.5	0.3	0.15	0.05	-0.1	-0.2	-0.3	-0.45
	↖ Same ↗															
	low dose				high dose				low dose				high dose			

Supplementary Table 1.

Parameters for plotting Fig.1c. To see the typical growth curves representing viability as a function of time in either cell death-dominant or senescence-dominant conditions, it was assumed that k_d or s was increased gradually while k_p decreased. The resulting proliferating-growth-rate $k = k_p - k_d - s$ decreased but had the same value for two conditions to assess different contributions of two mechanisms onto an overall growth behavior.

	Measurement	Metric evaluation	Final value	Response classification
a. Viability	End-point cell count $N_{viable}(C, t_e)$ (in full concentration range)	**viability=** $\frac{N_{viable}(C,t_e)}{N_{viable}(0,t_e)}$	IC50 (from dose-response curve)	Sensitive vs. resistance
b. GR-metric	End-point cell count $N_{viable}(C, t_e)$ (in full concentration range)	**GR=**$2^{\frac{\log N_{viable}(C,t_e)}{\log N_{viable}(0,t_e)}} - 1$	GR50 (from dose-response curve)	Sensitive vs. resistance
	Kinetics of cell count $N_{viable}(C, t)$ (in full concentration range)	**Model fitting** $e^{k't}$ $\rightarrow \quad k'(C) \quad \rightarrow$ **GR=**$2^{\frac{k'(C)}{k'(0)}} - 1$		
c. Phenotype-metric	Kinetics of cell count $N_{viable}(C, t)$ or $N_d(C, t)$ & End-point phenotype-fraction Senescent cell: $\frac{N_s}{N_p - N_0 + N_s}$ Dead cell: $\frac{N_d}{N_p - N_0 + N_s + N_d}$ (in clinically relevant range)	**Model fitting** $Ae^{kt} + (1 - A)$ or $B(e^{kt} - 1)$ $\rightarrow k(C) = k_p - k_d - s$ **Phenotype-fraction** $\frac{N_s}{N_p - N_0 + N_s} = \frac{s}{k_p - k_d}$ & $\frac{N_d}{N_p - N_0 + N_s + N_d} = \frac{k_d}{k_p}$ $\rightarrow$ $\boldsymbol{k_p}$, $\boldsymbol{k_d}$, and $\boldsymbol{s}$	$\frac{k_p(C)}{k_p(0)}$ ---------- $\frac{k_p(C) - k_p(0)}{k_p(0)}$ $\frac{k_d(C) - k_d(0)}{k_p(0)}$ $\frac{s(C) - s(0)}{k_p(0)}$	Sensitive vs. resistance ---------- Delayed-cell-division vs. Cell-death vs. Senescence

Supplementary Table 2.

The evaluation steps of the different drug-response metrics. The first step is the measurements of viable cell counts, or additionally phenotype fractions. The measurements are evaluated (a, b) to a full range dose-response curve for the conventional metrics or (c) to phenotype parameters for the phenotype metric. Measurements of the conventional metrics need to cover a full concentration range for a robust determination of IC50 or GR50. In contrast, for the phenotype-metric, a single or a few evaluations in a typical concentration range are enough to determine the drug potency and the dominant mechanism underlying growth inhibition. Herein, cell counts are normalized to its initial count N_0.

Cell line	Conc. (uM)	Fold change		a. Viability	
		at day 3	at day 6	**at day3**	**at day6**
OV1369(R2)	0.0	3.770	14.048	1.000	1.000
	1.0	2.605	8.021	0.691	0.571
	2.5	2.133	4.027	0.566	0.287
	5.0	1.878	2.982	0.498	0.212
	10.0	1.467	1.372	0.389	0.098
	15.0	1.476	1.220	0.392	0.087
OV1946	0.0000	5.234	27.554	1.000	1.000
	0.0025	4.638	21.890	0.886	0.794
	0.0050	4.463	17.250	0.853	0.626
	0.0100	3.382	6.894	0.646	0.250
	0.1000	2.638	3.890	0.504	0.141
	0.2500	2.204	2.200	0.421	0.080
	1.0000	1.132	1.566	0.216	0.057

		b. Growth-rate(GR) based metric											
		end point calculation		**simple exponential** fitting (**3 days** fitting)					**simple exponential** fitting (**6 days** full fitting)				
		GR (day3)	GR (day6)	apparent *k*(c)	std.error	t-value	p-value	**GR (day3)**	apparent *k*(c)	std.error	t-value	p-value	**GR (day6)**
OV1369(R2)	0.0	1.000	1.000	0.432	0.005	78.570	1.204E-17	1.000	0.445	0.001	487.717	1.792E-49	1.000
	1.0	0.649	0.727	0.306	0.005	60.314	2.853E-16	0.634	0.343	0.002	218.204	4.312E-41	0.707
	2.5	0.485	0.441	0.260	0.003	78.320	1.251E-17	0.517	0.247	0.002	118.704	9.422E-35	0.468
	5.0	0.390	0.332	0.232	0.007	34.266	2.429E-13	0.450	0.195	0.003	65.575	1.381E-28	0.356
	10.0	0.222	0.086	0.153	0.006	24.720	1.161E-11	0.278	0.088	0.007	13.487	1.074E-12	0.148
	15.0	0.226	0.054	0.152	0.007	22.572	3.382E-11	0.277	0.071	0.008	8.747	6.274E-09	0.118
OV1946	0.0000	1.000	1.000	0.541	0.006	96.676	1.003E-18	1.000	0.562	0.002	298.238	2.393E-44	1.000
	0.0025	0.901	0.906	0.488	0.009	56.285	6.524E-16	0.868	0.525	0.002	279.417	1.143E-43	0.910
	0.0050	0.871	0.813	0.489	0.006	78.848	1.154E-17	0.872	0.486	0.002	251.980	1.365E-42	0.820
	0.0100	0.666	0.497	0.393	0.006	67.419	7.527E-17	0.655	0.348	0.005	71.018	2.057E-29	0.537
	0.1000	0.501	0.328	0.331	0.005	64.301	1.327E-16	0.528	0.263	0.006	43.021	3.140E-24	0.383
	0.2500	0.392	0.179	0.290	0.008	37.772	7.622E-14	0.451	0.179	0.010	18.722	7.967E-16	0.247
	1.0000	0.053	0.098	0.107	0.020	5.266	1.990E-04	0.148	0.060	0.007	8.992	3.752E-09	0.077

		c. Phenotype-metric									
		Metric1. Overall growth rate by kinetic measurement				Metric2. Phenotype fractions		Resulting parameters			
		$k(c)=k_p-k_d-s$	std.error	t-value	p-value	k_d/k_p	s/k_p	k_p	kd	s	
OV1369(R2)	0.0	0.438	0.008	55.540	5.185E-26	0.036	0.024	0.466	0.017	0.011	
	1.0	0.343	0.015	23.575	1.304E-17						
	2.5	0.171	0.016	11.002	1.224E-10	0.073	0.238	0.249	0.018	0.059	
	5.0	0.029	0.014	2.072	4.971E-02						
	10.0					0.277	1.661				
	15.0					0.483	1.991				
								-46.625	0.251	10.341	% Change compared to k1(c=0)
OV1946	0.0000	0.534	0.013	40.147	4.467E-22	0.054	0.010	0.570	0.031	0.006	
	0.0025	0.529	0.014	38.535	1.087E-21						
	0.0050	0.451	0.011	41.334	2.373E-22						
	0.0100	0.202	0.024	8.418	2.507E-08	0.440	0.067	0.410	0.180	0.027	
	0.1000	0.031	0.026	1.181	2.504E-01	0.401	0.127				
	0.2500					0.551	0.216				
	1.0000										
								-28.112	26.259	3.807	% Change compared to k1(c=0)

Supplementary Table 3.

The evaluation results of the different drug-response metrics. Each drug-response metric was evaluated with the public data of OV1369(R2) and OV1946 cell lines for Olaparib treatment according to the steps in Supplementary Table 2.

SUPPLEMENTARY NOTE

The general case for the phenotype model of drug-response.

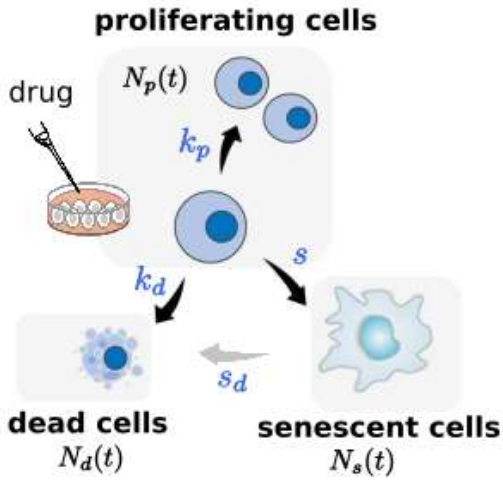

The coupled ordinary differential equations based phenotypic model for drug-response are

$$\frac{dN_p(t)}{dt} = k_p N_p(t) - k_d N_p(t) - s N_p(t)$$

$$\frac{dN_s(t)}{dt} = s N_p(t) - s_d N_s(t)$$

$$\frac{dN_d(t)}{dt} = k_d N_p(t) + s_d N_s(t)$$

In case that all of the parameters are not zero and the initial condition is $N_p(0) = N_0$, $N_s(0) = N'_0$, the full analytical solutions for each phenotype cell counts are;

$$N_p(t) = N_0 e^{(k_p - k_d - s)t}$$

$$N_s(t) = N_0 \frac{s}{k_p - k_d - s + s_d}\left(e^{(k_p - k_d - s)t} - e^{-s_d t}\right) + N'_0 e^{-s_d t}$$

$$N_d(t) = N_0 \frac{k_d(k_p - k_d - s + s_d) + s s_d}{(k_p - k_d - s + s_d)(k_p - k_d - s)}\left(e^{(k_p - k_d - s)t} - 1\right) + \left(N_0 \frac{s}{k_p - k_d - s + s_d} - N'_0\right)(e^{-s_d t} - 1)$$

This simple model holds regardless of the existence of other cell death mechanisms because the overall shape of differential equations and resulting solutions don't change. In this case, k_d is the total rate of changes for cell death; $k_d = k_{\text{apoptosis}} + k_{\text{ferroptosis}} + \cdots$.